## SUPPLEMENTAL MATERIAL

**Guo et al., http://www.jem.org/cgi/content/full/jem.20101568/DC1**

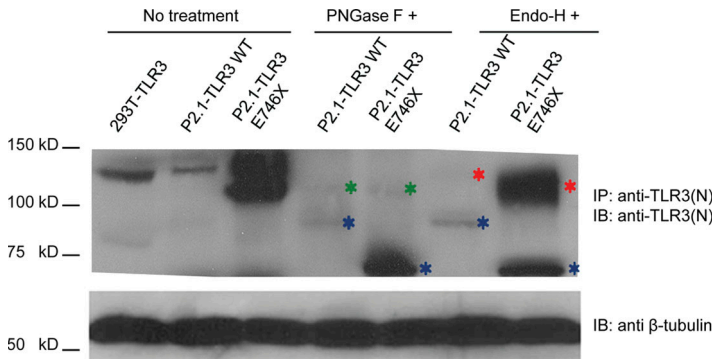


**Figure S1. Production of E746X TLR3 protein in P2.1 cells.** TLR3 protein levels were assessed by Western blotting in P2.1 TLR3-deficient fibrosarcoma cells transfected with WT *TLR3* (P2.1-TLR3 WT) or E746X (P2.1-TLR3 E746X) mutant *TLR3*, with an anti-TLR3 antibody. The proteins were not treated or were treated with PNGase F or Endo-H for 12 h. TLR3 protein extracted from HEK293T cells transfected with human WT *TLR3* was included as a positive control. We used β-tubulin as an internal expression control for Western blotting. Green asterisks indicate nonspecific bands, red asterisks indicate Endo-H–resistant bands, and blue asterisks indicate Endo-H–sensitive bands. The results shown are representative of two independent experiments. IB, immunoblot; IP, immunoprecipitation.

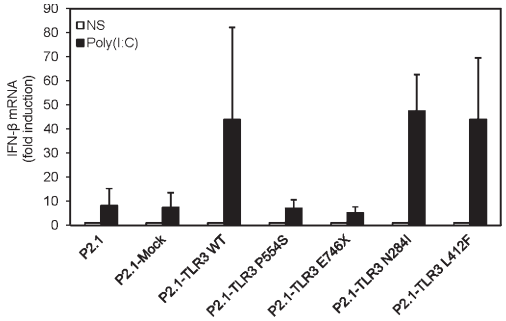


**Figure S2. The P554S and E746X *TLR3* alleles are loss-of-function.** IFN-β mRNA induction, unstimulated (NS) or after 2 h of stimulation with poly(I:C), assessed by RT-qPCR in P2.1 TLR3-deficient fibrosarcoma cells not transfected (P2.1) or transfected with WT *TLR3* (P2.1-TLR3 WT), P554S (P2.1-TLR3 P554S) or E746X (P2.1 TLR3 E746X) mutant *TLR3*, N284I (P2.1-TLR3 N284I) or L412F (P2.1-TLR3 L412F) *TLR3* variant, or mock vector (P2.1-mock). All transfections generated stable cell lines. β-Glucuronidase was included for normalization. The results shown are representative of two independent experiments. Mean values ± SD were calculated from triplicates in one experiment.

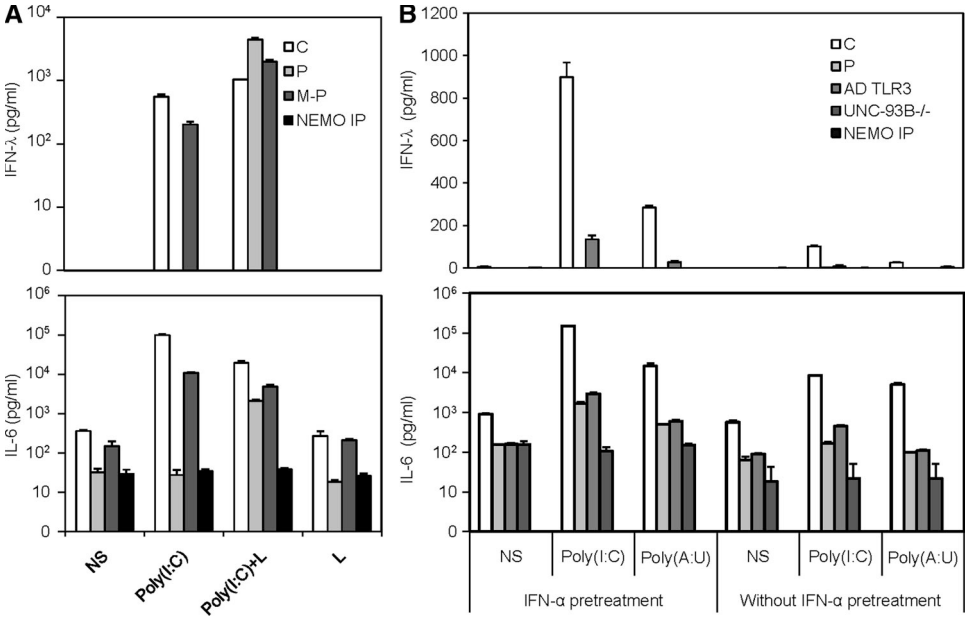


**Figure S3. Absence of response to TLR3 in the patient's fibroblasts.** (A) IFN-λ (top) and IL6 (bottom) production, left unstimulated (NS) or after poly(I:C) stimulation for 24 h with the presence of Lipofectamine (poly(I:C)+L) or without Lipofectamine (poly(I:C)), in primary fibroblast cells from a healthy control (C), the patient (P), the patient's mother (M-P), and a NEMO-deficient patient (NEMO IP) as assessed by ELISA. Mean values ± SD were calculated from the triplicates in one experiment, representative of three performed. (B) IFN-λ (top) and IL6 (bottom) production, unstimulated (NS) or after poly(I:C) or poly(A:U) stimulation for 24 h, in SV40-fibroblasts from a healthy control, the patient, a patient with AD TLR3 deficiency (AD TLR3), a patient with AR UNC-93B deficiency (UNC-93B$^{-/-}$), and a NEMO-deficient patient (MENO IP). The cells were not treated (right) or were subjected to prior treatment (left) with recombinant IFN-α2b for 18 h. Mean values ± SD were calculated from triplicates in one experiment, representative of two performed.

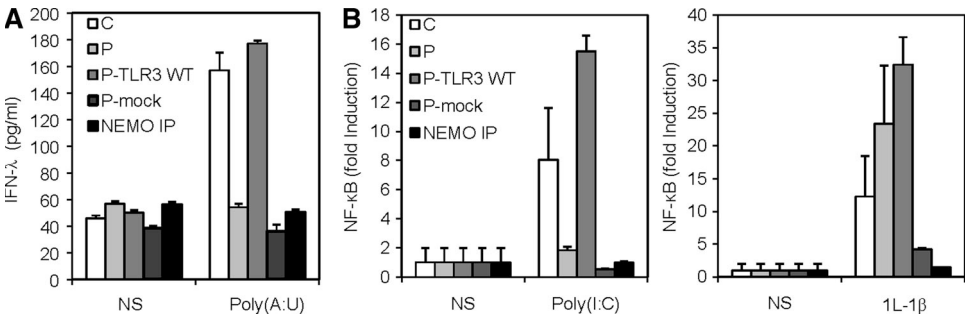


**Figure S4. TLR3 responsiveness is rescued by WT TLR3 expression in the patient's fibroblasts.** (A) IFN-λ production after stimulation with poly(A:U) or left unstimulated (NS), as assessed by ELISA, in SV40-fibroblasts from a control (C), a NEMO-deficient patient (NEMO IP), and P, and in SV40-fibroblasts from P transfected with an empty vector (P-mock) or C-terminally HA-tagged pUNO-TLR3 WT vector (P-TLR3 WT). All transfections generated stable cell lines. Mean values ± SD were calculated from triplicates in one experiment, representative of three independent experiments performed. (B) NF-κB activation was assessed with the NF-κB luciferase reporter without stimulation or upon stimulation with poly(I:C) (left) and IL-1β (right) for 6 h in SV40-fibroblasts from a control, a NEMO-deficient patient (NEMO IP) and the patient (P), and in SV40-fibroblasts from P transfected with an empty vector (P-mock) or C-terminally HA-tagged pUNO-TLR3 WT vector (P-TLR3 WT). All transfections generated stable cell lines. The panels illustrate mean values ± SD and the results shown are representative of three independent experiments.

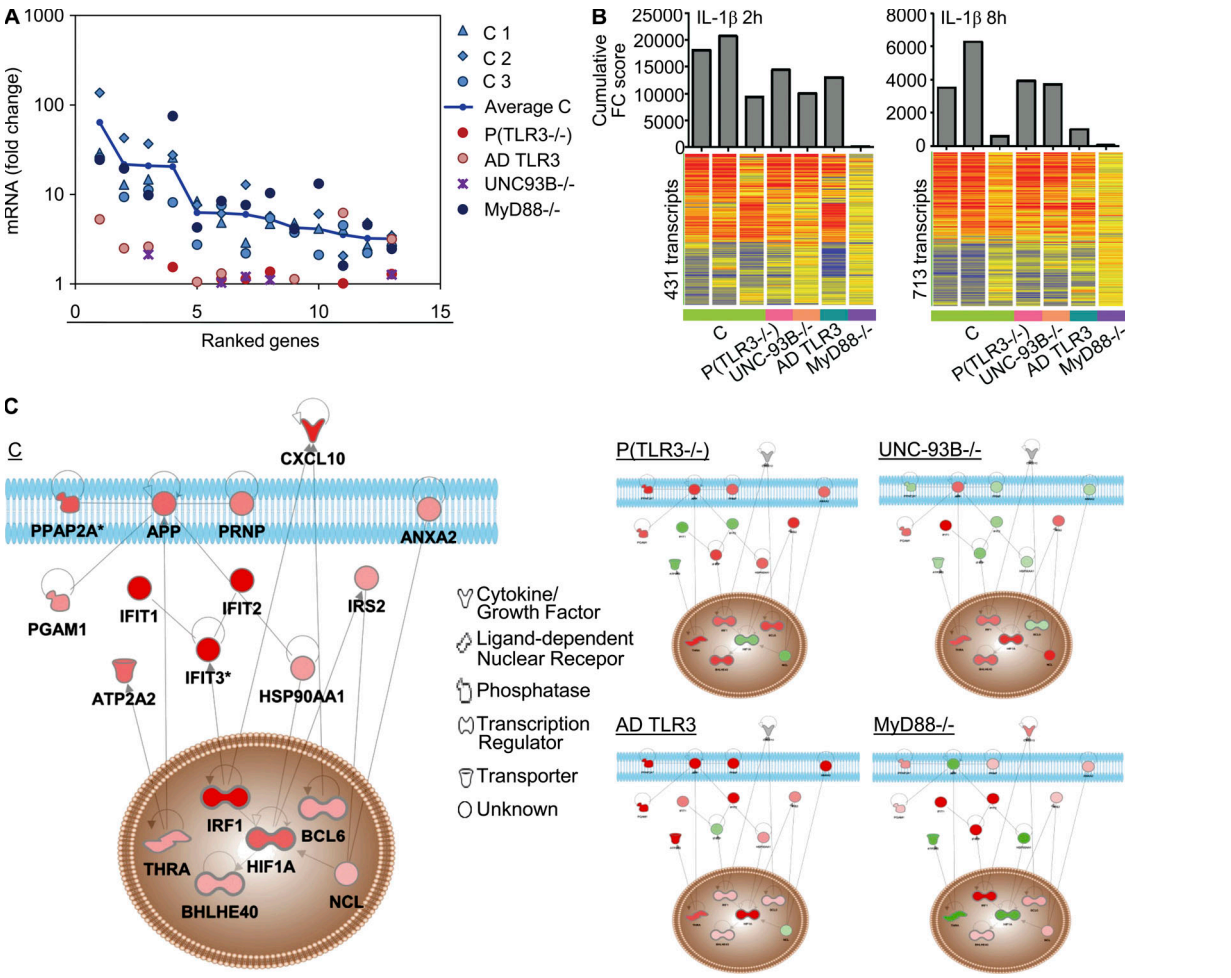


**Figure S5. Genome-wide transcriptional evaluation of the TLR3 pathway in fibroblasts.** (A) Ranking of the 13 transcripts up-regulated, with a fold change of at least 2 in all three controls tested, in primary fibroblasts from three healthy controls (C), the patient (P), one UNC-93B$^{-/-}$ patient, one AD TLR3-deficient patient, and one MyD88$^{-/-}$ patient after 2 h of poly(I:C) stimulation. (B) Cumulative fold change (FC) score (top) and heat maps (bottom) of the transcripts regulated by 2 h (left) or 8 h (right) of stimulation with IL-1β in primary fibroblasts from three healthy controls, the patient, one UNC-93B$^{-/-}$ patient, one patient with AD TLR3 deficiency (AD TLR3), and one patient with MyD88 deficiency (MyD88$^{-/-}$). The cumulative fold change score is the sum of all the fold change values >1.5 (up- or down-regulation). Heat maps represent a hierarchical clustering of transcripts differentially expressed upon poly(I:C) stimulation (based on a difference of 100 in intensity and a 1.5-fold change with respect to baseline in healthy controls). Changes with respect to nonstimulated conditions are represented by a color scale: red, up-regulated; blue, down-regulated; yellow, no change. Probes yielding a difference in intensity >100 were used to calculate the cumulative score. (C) Networks generated from differentially expressed transcripts (up-regulated) in control fibroblasts (C) and fibroblasts from the patient (P), one UNC-93B$^{-/-}$ patient, one AD TLR3-deficient patient, and one MyD88$^{-/-}$ patient after 2 h of poly(I:C) stimulation with Ingenuity Pathway Analysis software. Eligible genes or gene products regulated by these factors are represented as nodes, and the biological relationship between two nodes is represented as an edge (line). Solid and dashed lines indicate direct and indirect relationships, respectively. All edges are supported by at least one reference from the literature. Nodes are arranged according to the cellular distribution of the corresponding gene products. Up-regulated transcripts are represented in red, and down-regulated transcripts in are represented in green.

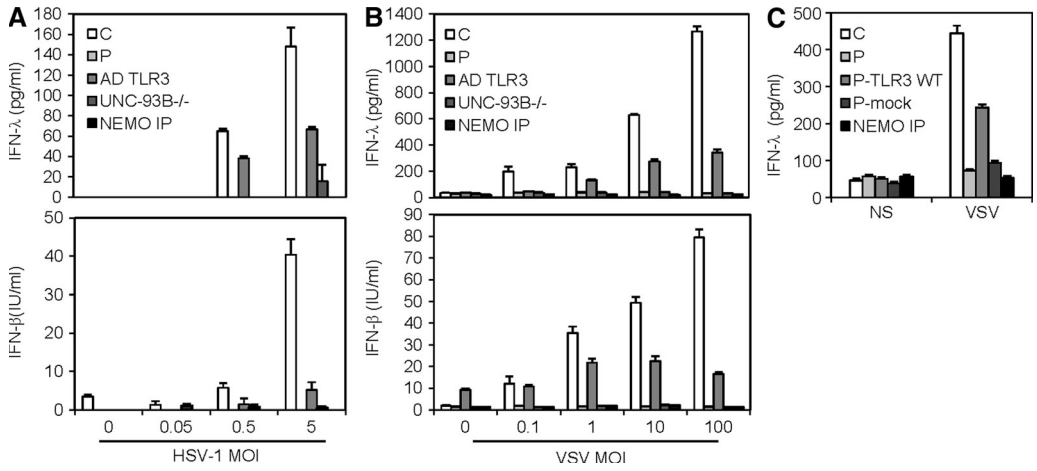


**Figure S6. Impaired production of IFN by the patient's fibroblasts upon HSV-1 or VSV infection.** (A) Production of IFN-λ (top) and IFN-β (bottom) after stimulation with HSV-1 at various MOIs, as assessed by ELISA, in SV40-fibroblasts from a control (C), the patient (P), an AD TLR3-deficient patient (AD TLR3), a UNC-93B$^{-/-}$ patient, and a NEMO IP patient. The panels illustrate results from a single experiment, representative of three performed. Mean values ± SD were calculated from triplicates in one experiment. (B) Production of IFN-λ (top) and IFN-β (bottom) after stimulation with VSV at various MOIs, as assessed by ELISA, in SV40-fibroblasts from a control, the patient, an AD TLR3 patient, a UNC-93B$^{-/-}$ patient, and a NEMO IP patient. The panels illustrate results from a single experiment, representative of three performed. Mean values ± SD were calculated from triplicates in one experiment. (C) IFN-λ production, unstimulated (NS) or after 24 h of stimulation with VSV, as assessed by ELISA, in SV40-fibroblasts from a control, a NEMO-deficient patient (NEMO IP), the patient, and SV40-fibroblasts from the patient transfected with an empty vector (P-mock) or C-terminally HA-tagged pUNO-TLR3 WT vector (P-TLR3 WT). All transfections generated stable cell lines. Mean values ± SD were calculated from triplicates in one experiment, representative of three independent experiments performed.

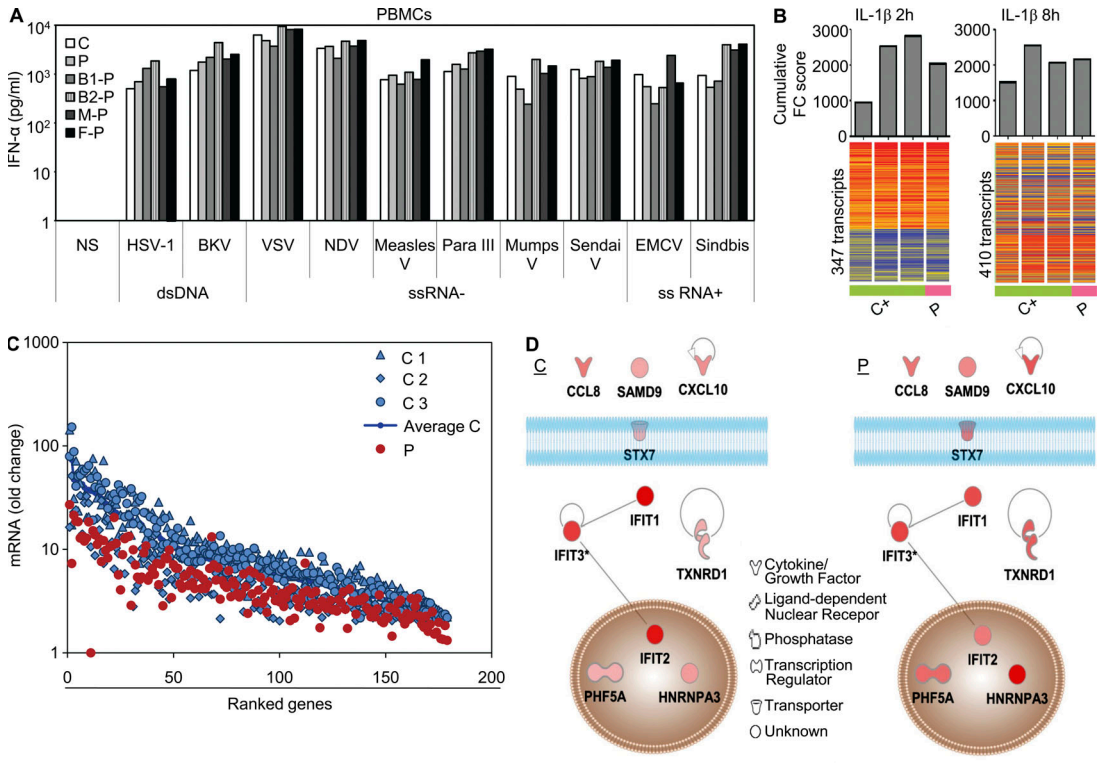


**Figure S7. Normal IFN production by the patient's PBMCs upon stimulation with various viruses and genome-wide transcriptional evaluation of poly(I:C) responses in PBMCs.** (A) IFN-α production after 24 h of stimulation with various viruses, or left unstimulated (NS), as measured by ELISA, in PBMCs from a positive control (C), the patient (P), his two siblings (B1-P, B2-P), his mother (M-P), and his father (F-P). The panel illustrates results from a single experiment, representative of two performed. (B) Cumulative fold change (FC) score (top) and heat maps (bottom) of the transcripts regulated by 2 h (left) or 8 h (right) of stimulation with IL-1β in PBMCs from three healthy controls and the patient. The cumulative fold change score is the sum of all the fold change values >1.5 (up- or down-regulation). Heat maps represent a hierarchical clustering of transcripts differentially expressed upon poly(I:C) stimulation (based on a difference of 100 in intensity and a 1.5-fold change with respect to baseline in healthy controls). Changes with respect to nonstimulated conditions are represented by a color scale: red, up-regulated; blue, down-regulated; yellow, no change. Probes yielding a difference >100 were used to calculate the cumulative score. (C) Ranking of the 179 transcripts up-regulated, with a fold change of at least 2 in all three controls tested, in PBMCs from three healthy controls and the patient after 8 h of poly(I:C) stimulation. (D) Networks generated from differentially expressed transcripts (up-regulated) in control and patient PBMCs after 2 h of poly(I:C) stimulation with Ingenuity Pathway Analysis software. Eligible genes or gene products regulated by these factors are represented as nodes, and the biological relationship between two nodes is represented as an edge (line). Solid and dashed lines indicate direct and indirect relationships, respectively. All edges are supported by at least one reference from the literature. Nodes are arranged according to the cellular distribution of the corresponding gene products. Up-regulated transcripts are represented in red.

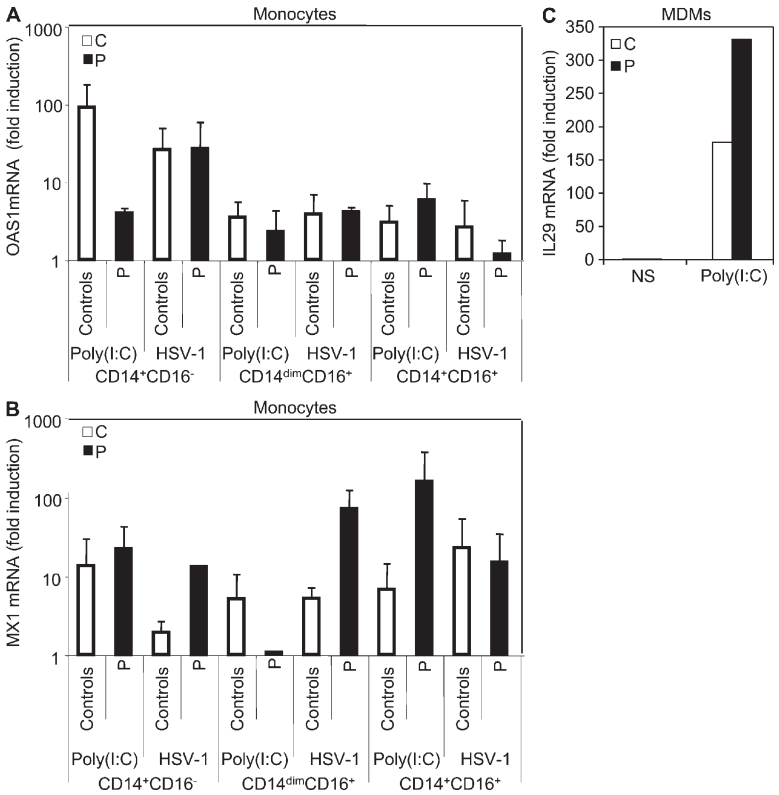


**Figure S8. Normal IFN production by the patient's leukocytes upon stimulation with poly(I:C) or HSV-1.** (A and B) Induction of OAS1 (A) and MX1 (B) mRNA induction after 24 h of poly(I:C) or HSV-1 stimulation in $CD14^+CD16^-$, $CD14^{dim}CD16^+$, and $CD14^+CD16^+$ monocytes from three healthy controls (C) and the patient (P) at a cell density of $10^4$cells/well. Bars represent fold change as compared with unstimulated (means ± SD). GAPDH was used for normalization. OAS1 and MX1 RT-qPCR assays were repeated twice with cDNA samples from one experiment. (C) Induction of IL29 mRNA after 4 h of poly(I:C) stimulation, or left unstimulated (NS), in MDMs from a healthy control and the patient.

**Table S1.** Number of transcripts differentially expressed upon stimulation with poly(I:C) or IL-1β in control fibroblasts

| Stimulations | Up-regulated | Down-regulated | Total |
|---|---|---|---|
| poly(I:C) 2 h | 202 | 117 | 319 |
| poly(I:C) 8 h | 713 | 637 | 1,350 |
| IL-1β 2 h | 247 | 184 | 431 |
| IL-1β 8 h | 398 | 315 | 713 |

**Table S2.** Number of transcripts differentially expressed upon stimulation with poly(I:C) or IL-1β in control PBMCs

| Stimulations | Up-regulated | Down-regulated | Total |
|---|---|---|---|
| poly(I:C) 2 h | 17 | 9 | 26 |
| poly(I:C) 8 h | 366 | 80 | 446 |
| IL-1β 2 h | 216 | 131 | 347 |
| IL-1β 8 h | 246 | 164 | 410 |

**Table S3.** In vivo viral infection in TLR3-deficient mice

| Virus | Mouse strain | Inoculation route | Phenotype | Reference |
|---|---|---|---|---|
| EMCV | 129SV | i.p. | Susceptible | Hardarson et al., 2007 |
| Mouse CMV | C57BL | i.p. | Susceptible | Tabeta et al., 2004; Edelmann et al., 2004 |
| Lymphocytic choriomeningitis virus | C57BL/6xB129 | i.p. and foot pad | Resistant as WT | Edelmann et al., 2004 |
| VSV | C57BL/6xB129 | intravenous | Resistant as WT | Edelmann et al., 2004 |
| Reovirus | C57BL/6xB129 | intracerebral or i.c. | Resistant as WT | Edelmann et al, 2004 |
| Respiratory syncytial virus | C57BL/6 | intratracheal | Susceptible | Rudd et al., 2006 |
| Influenza virus | C57BL/6 | i.n. | More resistant than WT | Le Goffic et al., 2006 |
| West Nile virus | C57BL/6 | i.p. and intracerebroventricular | More resistant than WT | Wang et al., 2004 |
| Punta toro virus | C57BL/6 | s.c. | More resistant than WT | Gowen et al., 2006 |
| Coxsackievirus B3 | C57BL/6 | i.p. | Susceptible | Negishi et al., 2008 |
| Coxsackievirus B4 | NOD/ShiLtJ | i.p. | Susceptible | Richer et al., 2009 |
| Vaccinia virus | C57BL/6 | i.n. | More resistant than WT | Hutchens et al., 2008 |

i.c., intracranial; i.n., intranasal.

## REFERENCES

Edelmann, K.H., S. Richardson-Burns, L. Alexopoulou, K.L. Tyler, R.A. Flavell, and M.B. Oldstone. 2004. Does Toll-like receptor 3 play a biological role in virus infections? *Virology*. 322:231–238. http://dx.doi.org/10.1016/j.virol.2004.01.033

Gowen, B.B., J.D. Hoopes, M.H. Wong, K.H. Jung, K.C. Isakson, L. Alexopoulou, R.A. Flavell, and R.W. Sidwell. 2006. TLR3 deletion limits mortality and disease severity due to Phlebovirus infection. *J. Immunol.* 177:6301–6307.

Hardarson, H.S., J.S. Baker, Z. Yang, E. Purevjav, C.H. Huang, L. Alexopoulou, N. Li, R.A. Flavell, N.E. Bowles, and J.G. Vallejo. 2007. Toll-like receptor 3 is an essential component of the innate stress response in virus-induced cardiac injury. *Am. J. Physiol. Heart Circ. Physiol.* 292:H251–H258. http://dx.doi.org/10.1152/ajpheart.00398.2006

Hutchens, M., K.E. Luker, P. Sottile, J. Sonstein, N.W. Lukacs, G. Núñez, J.L. Curtis, and G.D. Luker. 2008. TLR3 increases disease morbidity and mortality from vaccinia infection. *J. Immunol.* 180:483–491.

Le Goffic, R., V. Balloy, M. Lagranderie, L. Alexopoulou, N. Escriou, R. Flavell, M. Chignard, and M. Si-Tahar. 2006. Detrimental contribution of the Toll-like receptor (TLR)3 to influenza A virus-induced acute pneumonia. *PLoS Pathog.* 2:e53. http://dx.doi.org/10.1371/journal.ppat.0020053

Negishi, H., T. Osawa, K. Ogami, X. Ouyang, S. Sakaguchi, R. Koshiba, H. Yanai, Y. Seko, H. Shitara, K. Bishop, et al. 2008. A critical link between Toll-like receptor 3 and type II interferon signaling pathways in antiviral innate immunity. *Proc. Natl. Acad. Sci. USA*. 105:20446–20451. http://dx.doi.org/10.1073/pnas.0810372105

Richer, M.J., D.J. Lavallée, I. Shanina, and M.S. Horwitz. 2009. Toll-like receptor 3 signaling on macrophages is required for survival following coxsackievirus B4 infection. *PLoS ONE*. 4:e4127. http://dx.doi.org/10.1371/journal.pone.0004127

Rudd, B.D., J.J. Smit, R.A. Flavell, L. Alexopoulou, M.A. Schaller, A. Gruber, A.A. Berlin, and N.W. Lukacs. 2006. Deletion of TLR3 alters the pulmonary immune environment and mucus production during respiratory syncytial virus infection. *J. Immunol.* 176:1937–1942.

Tabeta, K., P. Georgel, E. Janssen, X. Du, K. Hoebe, K. Crozat, S. Mudd, L. Shamel, S. Sovath, J. Goode, et al. 2004. Toll-like receptors 9 and 3 as essential components of innate immune defense against mouse cytomegalovirus infection. *Proc. Natl. Acad. Sci. USA*. 101:3516–3521. http://dx.doi.org/10.1073/pnas.0400525101

Wang, T., T. Town, L. Alexopoulou, J.F. Anderson, E. Fikrig, and R.A. Flavell. 2004. Toll-like receptor 3 mediates West Nile virus entry into the brain causing lethal encephalitis. *Nat. Med.* 10:1366–1373. http://dx.doi.org/10.1038/nm1140